SCIENCE CHINA
Technological Sciences

• Article •

April 2016 Vol.59 No.4: 558–564
doi: 10.1007/s11431-015-5921-1

New high-accuracy spacecraft VLBI tracking using high data-rate signal: A demonstration with Chang'E-3

ZHOU Huan*, XU DeZhen, CHEN ShaoWu, LI HaiTao & DONG GuangLiang

Beijing Institute of Tracking and Telecommunications Technology, Beijing 100094, China

Received May 14, 2015; accepted August 17, 2015; published online September 9, 2015

As the scientific data volume in deep-space exploration rapidly grows, spacecraft heavily relies on high data-rate signals that span several megahertz to transmit data back to Earth. Employing high data-rate signals for high-accuracy radiometric interferometry can simultaneously deal with data transmission and spacecraft navigation. We demonstrate very long baseline interferometry (VLBI) tracking of the Chang'E-3 lander and rover to determine their relative lunar-surface position using downlink high data-rate signals. A new method based on the VLBI phase-referencing technique is proposed to obtain the differential phase delay, which is much more accurate than the differential group delay acquired by conventional VLBI approaches. The systemic errors among different signal channels have been well calibrated using the new method. The data from the Chang'E-3 mission were then processed, and meter-level accuracy positions of the rover with respect to the lander have been obtained. This demonstration shows the feasibility of high-accuracy radiometric interferometry using high data-rate signals. The method proposed in this paper can also be applied to future deep-space navigation.

spacecraft VLBI tracking, high data-rate signal, differential phase delay, Chang'E-3, deep-space navigation

Citation: Zhou H, Xu D Z, Chen S W, et al. New high-accuracy spacecraft VLBI tracking using high data-rate signal: A demonstration with Chang'E-3. Sci China Tech Sci, 2016, 59: 558–564, doi: 10.1007/s11431-015-5921-1

1 Introduction

Deep-space exploration bridges human beings with the unknown outer space. Many interplanetary spacecraft are now investigating mysterious unknowns and generate a large amount of scientific data. The growing data volume requires much more high-capacity downlink than ever before, which will take more time for a spacecraft to send out high data-rate signals back to the ground in a restricted bandwidth. Meanwhile, accurate spacecraft navigation is also indispensable for mission security and science objectives. Ranging, Doppler, and radiometric interferometry are the three basic techniques used for spacecraft navigation [1]. Ranging is employed to obtain the distance between a spacecraft and a ground station, and Doppler obtains the change rate in the distance. They are sensitive to the spacecraft movements along the line-of-sight direction. On the other hand, radiometric interferometry, which is sensitive to movements in the plane-of-sky, obtains the angular position of a spacecraft by measuring the signal arrival-time delay between two widely separated tracking stations, which is also referred to as very long baseline interferometry (VLBI) [2]. VLBI measurements are less sensitive to non-modeled spacecraft acceleration and provide important supplements for ranging and Doppler.

The time delay of VLBI measurement is calculated from the correlation results of the signals received by two stations. The wider the bandwidth of the signals is, the more accurate the time delay is. In addition, to reduce the measurement errors arising from such sources as atmospheric perturbations, station location uncertainties, and instrument errors, a

*Corresponding author (email: zhouhuan@bittt.cn)

nearby reference quasar with a well-known position is alternately observed to correct the time delay of the spacecraft. Then, we can obtain the differential delay between the two sources and determine their relative angular separation, which is the basis of the delta VLBI (ΔVLBI). However, using a high data-rate signal over a bandwidth of several megahertz from a spacecraft only allows us to acquire the differential group delay from conventional ΔVLBI, which is not sufficiently accurate to satisfy the mission requirements [3]. To improve the delay accuracy, another technique called delta differential one-way range (ΔDOR) has been investigated [4]. By transmitting several wide spanning beacons from a spacecraft, this technique can expand the signal bandwidth span to approximately 40 MHz at the X band, and the differential group delay accuracy could reach several hundred picoseconds. Nevertheless, beacon transmission usually disrupts the transmission of scientific data because of limited downlink power and spectrum management requirements.

In this paper, we present a high-accuracy VLBI tracking experiment conducted for the Chang'E-3 lander and rover using their high data-rate signals. The lander is selected as the reference source, and the position of the rover on the lunar surface relative to the lander needs to be determined [5,6]. To obtain a much more accurate differential phase delay instead of a differential group delay, a method based on the VLBI phase-referencing technique is developed. Without requiring beacon measurements, the VLBI phase-referencing technique can operate with all types of spacecraft signals and resolve the phase ambiguities in the space-time domain, leading to a 10-ps-level differential phase delay [7,8]. This method has been tested by the National Aeronautics and Space Administration and European Space Agency [9–11]. A previous VLBI phase-referencing experiment in the Chang'E-3 mission demonstrated the feasibility of spacecraft tracking utilizing a narrowband low data-rate telemetry signal from the rover [12]. However, some new problems arise when we use the high data-rate signal. The details of the problems are discussed in Section 2, and Section 3 describes our method. The experimental results are discussed in Section 4, followed by the accuracy analysis in Section 5 and conclusion in Section 6.

2 Data acquisition

Soon after touching down on the lunar surface, the rover was separated from the lander and moved around to take photographs of the lander at several planned sites during the first few days [13]. The lander sent the scientific and telemetry data to the ground using a high data-rate signal spanning 5 MHz at the X band. Meanwhile, the rover alternated between a 4-kHz low data-rate signal and a 4-MHz high data-rate signal. Most of the time, the low data-rate signal was selected, except for periods when it delivered the photographs back. These photo-transmission periods were no more than 1 h at every site in most cases. The telemetry, tracking, and command system of the Chang'E-3 mission assigned the ground VLBI stations to track the two probes using two 8-MHz-wide intermediate-frequency (IF) channels: the first one for the lander and the other one for the rover. The angular separation between the lander and rover was small enough for them to be observed by the same beam from a ground antenna. Four VLBI stations (Shanghai, Beijing, Kunming, and Urumqi) recorded the signals from the two probes and transmitted them to the Shanghai VLBI center via network for data correlation. More details of the observation and data correlation can be found in [12].

Figure 1 shows the interferometric fringes of the two probes. Figure 1(a) shows the cross-power spectra when the rover was sending out a low data-rate signal, and Figure 1(b) shows that when a high data-rate signal was being transmitted.

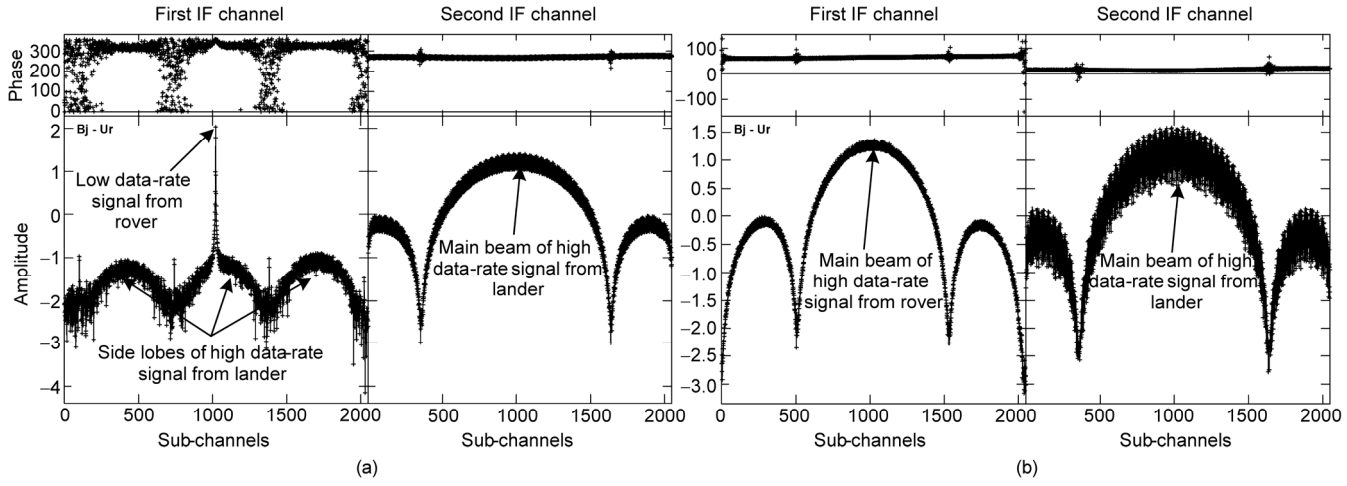

Figure 1 Cross-power spectra of the two probes via a 4096-point fast Fourier transform (a) when the rover transmits a low data-rate signal and (b) when the rover transmits high data-rate signal. The baseline ranges from Beijing (Bj) to Urumqi (Ur). The top panel of each IF channel shows the phase in units of degrees, and the bottom panel shows the signal amplitudes in logarithmic scale.

We can see the possibility of using only the data in the first IF channel to derive the differential delay between the low data-rate signal from the rover and the high data-rate signal from the lander because both signals were simultaneously recorded in the same IF channel. This process is actually what we have previously done [12]. However, if we want to derive the differential delay between the high data-rate signals from the rover and lander, the data in the first and second IF channels should be used together. Then, a problem arises, i.e., we experience unknown systemic delay errors between the two IF channels, and we have to calibrate the errors before calculating the differential delay. In general, a reference quasar should be regularly observed to perform this function using its ultra-wideband signals. However, in this demonstration, only two 1-h quasar observation scans were scheduled before and after the spacecraft tracking session, which usually lasted more than 8 h every day. Therefore, the delay errors, which varied during the spacecraft tracking, could not be accurately estimated using the two quasar observation scans.

3 Method

Instead of using a reference quasar, the lander can be employed to calibrate the delay errors among different IF channels. Figure 1(a) shows that when the rover was transmitting a low data-rate signal, the main beam of the lander high data-rate signal was recorded in the second IF channel. Meanwhile, its side lobes were also recorded in the first IF channel. The wideband signal generated clear interferometric fringes in both IF channels, which means that the lander can act as a reference quasar to correct the unknown delay errors.

According to the VLBI phase-referencing technique, the differential delay between the lander and rover should first be determined after the IF channel calibration. Then, a radio image of the rover is constructed. The offsets of the image peak intensity relative to the image center represent the angular separation between the lander and rover in the plane-of-sky. Afterward, the relative position of the rover with respect to the lander on the lunar surface could be determined.

By assuming that the rover sends out a low data-rate signal during t_0–t_1 and t_2–t_3, the side lobes of the lander high data-rate signal would be simultaneously included in the first IF channel. Here, its residual delay after the correlation is denoted as $\tau_L^D + \tau_{\mathrm{ch1}}$, where τ_L^D is the residual geometric delay corresponding to the high-gain antenna of the lander used to transmit the high data-rate signal and τ_{ch1} is the delay error in the first IF channel. By assuming that the rover sends out a high data-rate signal during t_1–t_2, only the rover high date-rate signal can now be seen in the first IF channel, and the relatively weak side lobes of the lander high data-rate signal are overshadowed. Similarly, the residual delay is denoted as $\tau_R^D + \tau_{\mathrm{ch1}}$, where τ_R^D is the residual geometric delay corresponding to the high-gain antenna of the rover. Because the lander transmits a high data-rate signal during t_0–t_3 for the whole time, only the lander high data-rate signal exists in the second IF channel over this period. The residual delay is denoted as $\tau_L^D + \tau_{\mathrm{ch2}}$, where τ_{ch2} is the delay error in the second IF channel. Figure 2 shows the data processing flowchart to extract the differential delay between the high data-rate signals from the two probes. The phase ambiguities, which are involved in the differential delay, will be automatically resolved in the imaging process with the help of the Earth rotation and a mix of baselines to derive the differential phase delay. The details of the process steps are as follows.

1) The correlated data are imported into the astronomical image processing system (AIPS) [14]. The low signal-to-noise ratio (SNR) side lobes of the lander high data-rate signal are flagged in the first IF channel during t_0–t_1 and t_2–t_3 as well as the rover low data-rate signal. The remaining high-SNR sub-channels, which are actually the useful parts of the lander high data-rate signal in the first IF channel, are fringe-fitted to obtain residual delay $\tau_L^D + \tau_{\mathrm{ch1}}$.

2) The fringe-fitting solutions obtained during t_0–t_1 and t_2–t_3 in Step 1 are applied to the lander high data-rate signal in the second IF channel, and the second IF channel are subsequently fringe-fitted, which means calculating $(\tau_L^D + \tau_{\mathrm{ch2}}) - (\tau_L^D + \tau_{\mathrm{ch1}})$. Therefore, the delay error difference $\tau_{\mathrm{ch2}} - \tau_{\mathrm{ch1}}$ between the two IF channels is derived.

3) The delay error differences during t_1–t_2 are interpolated using the solutions acquired from Step 2 during t_0–t_1 and t_2–t_3. The results are represented as $\tilde{\tau}_{\mathrm{ch2}} - \tilde{\tau}_{\mathrm{ch1}}$ and are applied to the signal in the second IF channel. The second IF channel is fringe-fitted again to calculate $(\tau_L^D + \tau_{\mathrm{ch2}}) - (\tilde{\tau}_{\mathrm{ch2}} + \tilde{\tau}_{\mathrm{ch1}})$. Considering that the variation in the delay error difference within a short time interval is quite small, the interpolation errors are ignored, and we can obtain $\tau_L^D - \tilde{\tau}_{\mathrm{ch1}}$.

4) The solutions from Step 3 are applied to the rover high data-rate signal in the first IF channel during t_1–t_2, which is equivalent to calculating $(\tau_R^D + \tau_{\mathrm{ch1}}) - (\tau_L^D + \tilde{\tau}_{\mathrm{ch1}})$. Then, the differential delay between the lander and rover during t_1–t_2 is determined.

5) The differentiated signal of the rover is exported from the AIPS and imported to the difference-mapping program [15]. The data are cleaned, and a radio image of the rover is constructed without self-calibration. The offsets of the image peak intensity in right ascension (RA) and declination (Dec) are measured and transformed into the lunar local

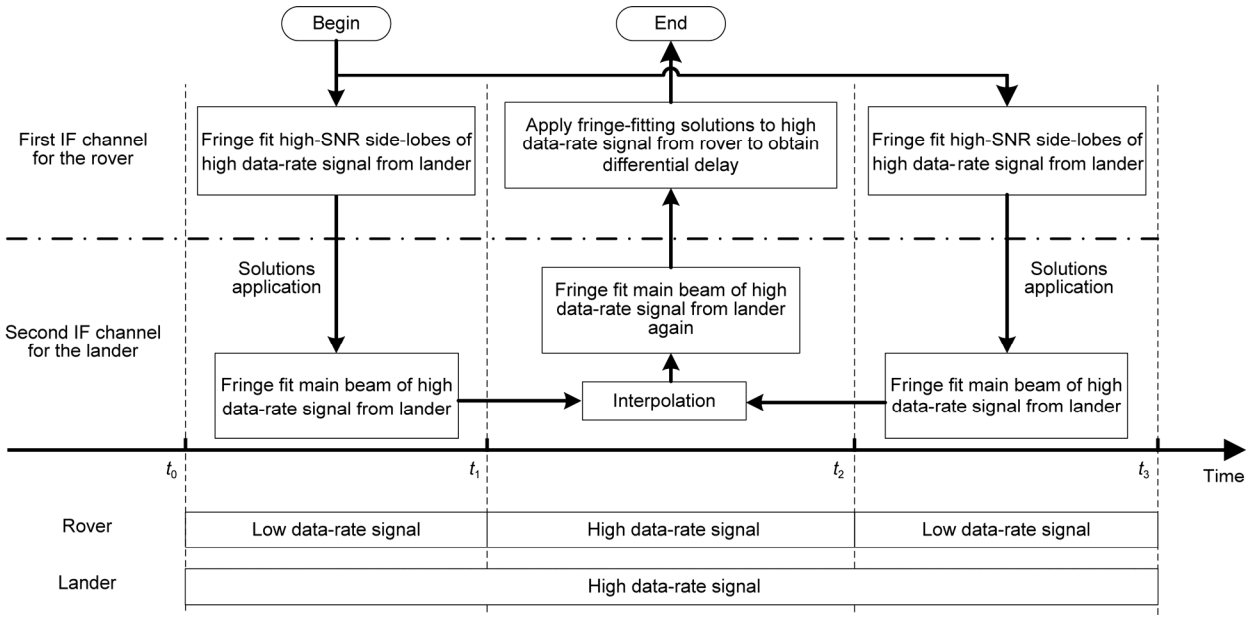

Figure 2 Data processing flowchart to extract the differential delay between the high data-rate signals from the two probes.

coordinate system of the lander to obtain the relative position of the rover on the lunar surface. Here, we assume that the height difference between the two probes is known in the coordinate transformation, as will be explained later.

4 Results

The observation data of Chang'E-3 on December 14, 15, and 21, 2014, were processed. We obtained the rover position relative to the lander at three sites. Figure 3 shows the images of the rover, and Table 1 lists the relative position results using our method and the traditional ΔVLBI technique. The high SNR of the high data-rate signal leads to good image qualities, although the observation scans were short and only four stations were available. The table also lists the epochs when the rover was sending out high data-rate signal and the reference values of the relative position. At the epoch on December 14, the rover was still located atop the lander before their separation. The height difference used to calculate the relative position and the reference value were read from the ground assembly diagram. Thus, this measurement provides a valuable result in evaluating the practical accuracy of the method. At the epochs on December 15 and 21, the rover was located at sites A and E, respectively. The two probes were supposed to be at the same height level, and the reference values were measured by visual localization technique with an accuracy of approximately 0.4 m [16,17]. We can see that the differences between our results and the reference values are less

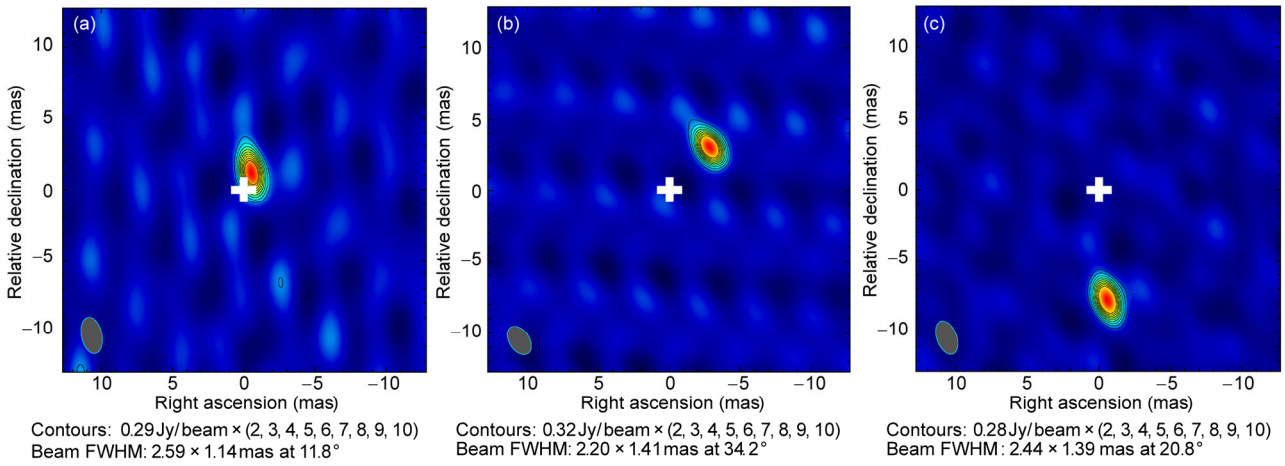

Figure 3 (Color online) Images of the rover on December (a) 14, (b) 15, and (c) 21, 2014. The image centers are marked with crosses. FWHM means full width at half maximum.

Table 1 Relative position measurements of the rover with respect to the lander

Date	Epoch (UTC)	VLBI phase referencing		ΔVLBI differential group delay		Reference value	
		North (m)	East (m)	North (m)	East (m)	North (m)	East (m)
14 Dec.	17:11:00–17:36:00 and 18:12:00–18:23:00	1.30	0.12	--	--	0.95	–0.05
15 Dec.	13:10:40–13:39:00 and 14:13:40–14:24:40	8.82	1.42	–4.24	0.43	9.03	1.50
21 Dec.	20:24:40–20:57:30 and 23:09:50–23:48:30	–19.11	–0.18	59.00	31.97	–19.77	–0.20

than 1 m, whereas the ΔVLBI measurements differ greatly from the reference values, demonstrating the feasibility and high-accuracy of radio interferometry using high data-rate signals with the VLBI phase-referencing technique. The relative positions in this study in terms of accuracy also agreed with those obtained from previous experiments using narrowband low data-rate signals [12] or the same-beam interferometry method [18].

To further investigate the performance of our method, we tried to measure the relative distance between the high-gain antenna of the rover, which is employed to transmit high data-rate signal, and its low-gain antenna, which is employed to transmit low data-rate signal. The positions of these two antennas have been differentiated. Table 2 lists the two measurement results on December 15 and 21. The height difference between the two antennas was 0.17 m. The reference value of the relative distance was obtained from the ground assembly diagram. The measurements were very close to the reference values because the data have been differentiated between two stations, two probes, and two antennas, canceling most of the measurement errors.

5 Error analysis

The VLBI phase referencing was developed to study remote quasars. For near-field spacecraft, the following measurement errors should be carefully considered.

5.1 Variation in the position vector from the lander to the rover in J2000.0 coordinate system

The position vector from the lander to the rover is invariable in the lunar local coordinate system when the rover stops at a certain site. However, in the geocentric equatorial inertial coordinate system J2000.0, where the separation between the two probes in RA and Dec are determined from the image, the vector changes with the motion of the Moon, which indicates that the relative position we obtain is the average during the observation scan. Therefore, we must know the magnitude of the variation in J2000.0. Figure 4 shows the simulation results when the rover was at site A on December 15 with the epoch ranging from 15:00 to 17:00. We can see that the variations in the three vector components are less than 0.2 m, and the angular separation seen from the Earth center is very stable, whereas the vectorial angle varies by approximately 0.5°. Because the mid-interval of the scan is chosen as the time instant when we transform the offsets in RA and Dec to the lunar local coordinate system, the measurement errors induced by this term would be less than 0.1 m.

5.2 Uncertainty of the lander location

In the coordinate transformation, the position of the lander is required. The lander location on the lunar surface has been determined with an accuracy of approximately 50 m using ranging, Doppler, and ΔDOR measurements [19]. Uncertainty in the lander location can result in relative position errors. We evaluated the effect of this term when the rover was at site A. The uncertainty of the lander location was supposed to be 0.02° in both longitude and latitude (~600 m on the lunar surface) and 100 m in altitude. Figure 5 shows the simulation results. The errors caused by the uncertainty were somewhat small. Hence, we do not have to take this term into account.

5.3 Height-difference error between the lander and rover

Determining the three-dimensional relative location of the rover is impossible if only the offsets between the two probes in RA and Dec are available. We assumed that the two probes were located at the same height level on

Table 2 Measurements of the distance between the high- and low-gain antennas of the rover

Date	Antenna	Relative position [a)]		Relative distance	
		North (m)	East (m)	Reference value (m)	Measurement (m)
15 Dec.	High gain	10.36	0.93	1.13	1.18
	Low gain	11.52	1.03		
21 Dec.	High gain	–17.53	–0.54	1.13	1.36
	Low gain	–18.84	–0.86		

a) Positions of the rover antennas relative to the lander high-gain antenna.

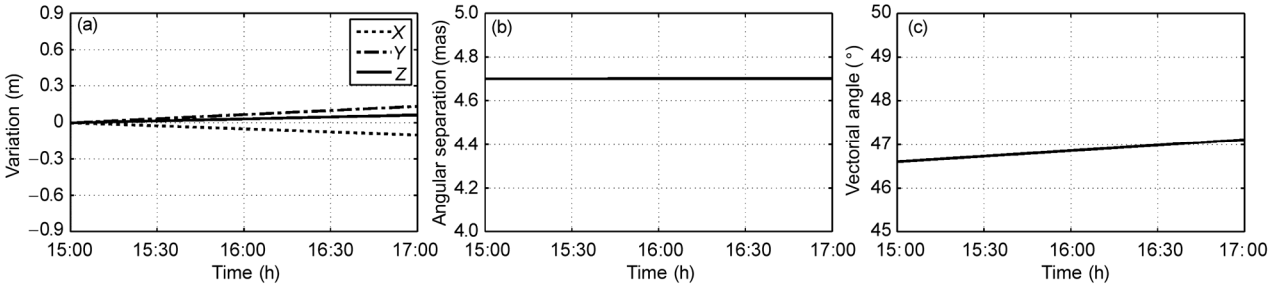

Figure 4 (a) Variations in the three components of the position vector; (b) Variation in the angular separation; (c) Variation in the angle between the position vector and direction of right accession.

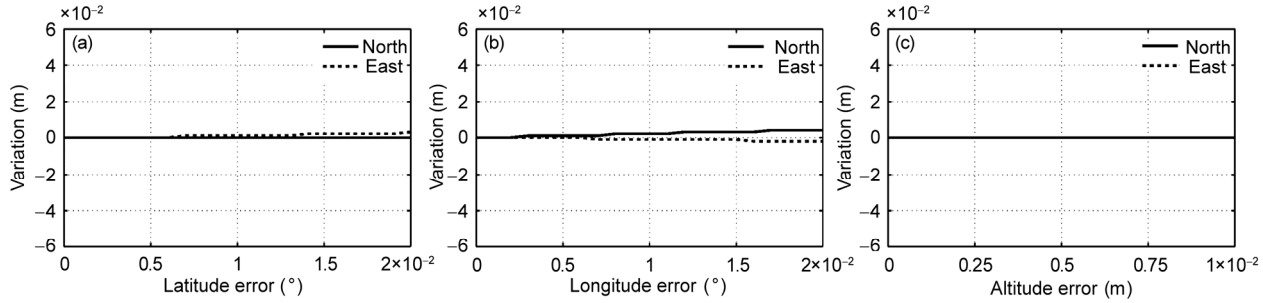

Figure 5 Variations in the relative position caused by the uncertainties in (a) latitude error, (b) longitude error, and (c) altitude error.

December 15 and 21 owing to the flat terrain. This approximation would greatly affect the results. Again, we considered the rover at site A as an example. Figure 6 shows the simulation with varying height-difference errors between the lander and rover. We can see that the variations in the relative positions in the north and east directions exceeded 0.6 m when the height-difference error reached 1 m. From the visual location results, we observed that the actual height-difference errors were much less than 1 m on December 15 and 21 [20]. Therefore, the position errors induced by this term are less than 0.5 m. However, the analysis demonstrated the importance in improving the height-difference accuracy. One method to achieve this is to add ranging and Doppler information, which can provide constraints in the line-of-sight direction but was not available for the current simple rover [21]. Another approach is to use the lunar topographic maps from the Lunar Orbiter Laser Altimeter data to obtain the height difference [22]. The possible accuracy using these new data should be further studied.

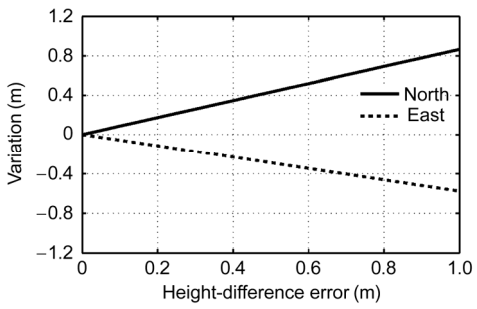

Figure 6 Variations in the relative position caused by the height-difference error.

Overall, in the demonstration, the relative positions of the rover with meter-level accuracy have been achieved. The differential phase delay accuracy of our results is equivalent to approximately 20 ps, which is approximately two orders of magnitude better than the differential group delay obtained from the ΔVLBI measurement.

6 Conclusion

A successful demonstration of radiometric interferometry using high data-rate signal has been presented in this paper. The feasibility of the new method for spacecraft VLBI tracking has been demonstrated. The systemic delay errors among the different IF channels in the Chang'E-3 mission were well calibrated, and the relative position between the lander and rover was determined with meter-level accuracy. Our results show the capabilities of high-accuracy interferometry without disrupting the scientific data transmission. Applying this method into future interplanetary missions is promising to obtain the accurate angular separation of a spacecraft with respect to a certain reference.

This work was supported by the Key Techniques Research Program of China's Lunar Exploration (Grant No. TY3Q20100009). The authors would like to thank FAN Min of the Beijing Institute of Tracking and Telecommunications Technology and JIANG DongRong, HUANG Yong, TONG

FengXian, ZHENG WeiMin, and LI PeiJia of the Shanghai Astronomical Observatory for their support.

1 Border J S, Lanyi G E, Shin D K. Radiometric tracking for deep space navigation. In: Proceedings of the 31st Annual AAS Guidance and Control Conference, Breckenridge, Colorado, 2008
2 Lanyi G E, Bagri D S, Border J S. Angular position determination of spacecraft by radio interferometry. P IEEE, 2007, 85: 2193–2201
3 Li P J, Huang Y, Chang S Q, et al. Positioning for the Chang'E-3 lander and rover using Earth-based observations (in Chinese). Chin Sci Bull (Chin Ver), 2014, 59: 3162–3173
4 Border J S. Innovations in delta differential one-way range: From Viking to Mars Science Laboratory. In: Proceedings of the 21st International Symposium on Space Flight Dynamics, Toulouse, France, 2009
5 Liu Q H, Chen M, Xiong W M, et al. Relative position determination of a lunar rover using high-accuracy multi-frequency same-beam VLBI. Sci China-Phys Mech Astron, 2010, 53: 571–578
6 Chen M, Liu Q H, Wu Y J, et al. Relative position determination of a lunar rover using the biased differential phase delay of same-beam VLBI. Sci China-Phys Mech Astron, 2011, 54: 2284–2295
7 Lanyi G E, Border J S, Benson J, et al. Determination of angular separation between spacecraft and quasars with the very long baseline array. JPL: Interplanetary Network Progress Report 42–162, 2005
8 Majid W, Bagri D. In-beam phase referencing with the deep space network array. JPL: Interplanetary Network Progress Report 42-169, 2007
9 Martin-Mur T J, Highsmith D E. Mars approach navigation using the VLBA. In: Proceedings of the 21st International Symposium on Space Flight Dynamics, Toulouse, France, 2009. 1–10
10 Jones D L, Fomalont E, Dhawan V, et al. Very long baseline array astrometric observations of the Cassini spacecraft at Saturn. Astron J, 2011, 141: 29–45
11 Duev D A, Calves G M, Pogrebenko S V, et al. Spacecraft VLBI and Doppler tracking: Algorithms and implementation. Astron Astrophys, 2012, 541: A43
12 Zhou H, Li H T, Dong G L. Relative position determination between Chang'E-3 lander and rover using in-beam phase referencing. Sci China Inf Sci, 2015, 58: 092201
13 Sun Z Z, Jia Y, Zhang H. Technological advancements and promotion roles of Chang'e-3 lunar probe mission. Sci China Tech Sci, 2013, 56: 2702–2708
14 Greisen E, Bridle A. AIPS Cookbook. USA: National Radio Astronomy Observatory, 2013
15 Taylory G. The Difmap Cookbook. Pasadena, CA: California Institute of Technology, 2013
16 Wu W R, Wang D Y, Xin Y, et al. Binocular visual odometry algorithm and experimentation research for the lunar rover (in Chinese). Sci Sin Inform, 2011, 41: 1415–1422
17 Wang B F, Zhou J L, Tang G S, et al. Research on visual localization method of lunar rover (in Chinese). Sci Sin Inform, 2014, 44: 452–460
18 Liu Q H, Zheng X, Huang Y, et al. Monitoring motion and measuring relative position of the Chang'E-3 rover. Radio Sci, 2014, 49: 1080–1086
19 Huang Y, Chang S Q, Li P J, et al. Orbit Determination of Chang'E-3 and positioning of the lander and the rover. Chin Sci Bull, 2014, 59: 3858–3867
20 Liu Z Q, Di K C, Peng M, et al. High precision landing site mapping and rover localization for Chang'e-3 mission. Sci China-Phys Mech Astron, 2015, 58: 019601
21 Kahn R D, Folkner W M, Edwards C D, et al. Position determination of a lander and rover at Mars with Earth-based differential tracking. JPL: The Telecommunications and Data Acquisition Progress Report 42-108, 1992
22 Kreslavsky M A, Head J W, Neumann G A, et al. Lunar topographic roughness maps from Lunar Orbiter Laser Altimeter (LOLA) data: Scale dependence and correlation with geologic features and units. Icarus, 2013, 226: 52–66